

Total Synthesis of the Quinone Epoxide Dimer (+)-Torreyanic Acid: Application of a Biomimetic Oxidation/Electrocyclization/Diels–Alder Dimerization Cascade¹

Chaomin Li,[†] Richard P. Johnson,[‡] and John A. Porco, Jr.*[†]

Contribution from the Department of Chemistry and Center for Methodology and Library Development, Boston University, 590 Commonwealth Avenue, Boston, Massachusetts 02215, and Department of Chemistry, University of New Hampshire, Durham, New Hampshire 03824

Received December 2, 2002; E-mail: porco@chem.bu.edu

Abstract: An asymmetric synthesis of the quinone epoxide dimer (+)-torreyanic acid (**48**) has been accomplished employing [4 + 2] dimerization of diastereomeric 2*H*-pyran monomers. Synthesis of the related monomeric natural product (+)-ambuic acid (**2**) has also been achieved which establishes the biosynthetic relationship between these two natural products. A tartrate-mediated nucleophilic epoxidation involving hydroxyl group direction facilitated the asymmetric synthesis of a key chiral quinone monoepoxide intermediate. Thermolysis experiments have also been conducted on a model dimer based on the torreyanic acid core structure and facile retro Diels–Alder reaction processes and equilibration of diastereomeric 2*H*-pyrans have been observed. Theoretical calculations of Diels–Alder transition states have been performed to evaluate alternative transition states for Diels–Alder dimerization of 2*H*-pyran quinone epoxide monomers and provide insight into the stereocontrol elements for these reactions.

Introduction

Recently, a number of novel compounds have been isolated from *Pestalotiopsis* spp., a fungal genus that is well-known for the production of numerous bioactive secondary metabolites, including Taxol.² In 1996 Lee and co-workers reported the impressive dimeric quinone epoxide torreyanic acid (**1**, Figure 1)³, produced by an endophytic fungus *Pestalotiopsis microspora* associated with the Florida torrey tree. This natural product was found to be 5–10 times more potent in cell lines that are sensitive to the protein kinase C (PKC) agonist, 12-*o*-tetradecanoyl phorbol-13-acetate (TPA), and showed G1 arrest of G0 synchronized cells (1–5 μg/mL). The biochemical target of the compound has not been fully elucidated, although initial studies have implicated the eukaryotic translation initiation factor EIF-4a as a possible molecular target.⁴ The related monomeric epoxyquinols,ambuic acid (**2**)⁵ and jesterone (**3**),⁶ were isolated from *Pestalotiopsis* and closely resemble cycloepoxydon (**4**), an inhibitor of the phosphorylation of the NF-κB inhibitory protein IκB, from fermentations of a deuteromycete strain.⁷ The

related epoxyquinoid dimers (+)-epoxyquinol A (**5**) and B (**6**) were recently isolated by Osada and co-workers from an uncharacterized fungus and were found to have potent antiangiogenic activity.⁸

In the original report on the isolation and structural characterization of torreyanic acid, a biosynthetic scheme for the synthesis of the natural product was proposed involving Diels–Alder dimerization⁹ of 2*H*-pyran monomers epimeric at C9 (C9') (Figure 2). In this *endo*-selective [4 + 2] cycloaddition,^{10,11} the two pentyl side chains are oriented away from one another in

- (7) (a) Gehrt, A.; Erkel, G.; Anke, H.; Anke, T.; Sterner, O. *Nat. Prod. Lett.* **1997**, *9*, 259. (b) Gehrt, A.; Erkel, G.; Anke, T.; Sterner, O. *J. Antibiot.* **1998**, *51*, 455.
- (8) For isolation and antiangiogenic activity of epoxyquinol A: (a) Kakeya, H.; Onose, R.; Koshino, H.; Yoshida, A.; Kobayashi, K.; Kageyama, S.-I.; Osada, H. *J. Am. Chem. Soc.* **2002**, *124*, 3496. Epoxyquinol B: (b) Kakeya, H.; Onose, R.; Yoshida, A.; Koshino, H.; Osada, H. *J. Antibiot.* **2002**, *55*, 829. For synthetic studies, see: (c) Li, C.; Bardhan, S.; Pace, E. A.; Liang, M.-C.; Gilmore, T. D.; Porco, J. A., Jr. *Org. Lett.* **2002**, *4*, 3267. (d) Shoji, M.; Yamaguchi, J.; Kakeya, H.; Osada, H.; Hayashi, Y. *Angew. Chem., Int. Ed.* **2002**, *41*, 3192. (e) Shoji, M.; Kishida, S.; Takeda, M.; Kakeya, H.; Osada, H.; Hayashi, Y. *Tetrahedron Lett.* **2002**, *43*, 9155.
- (9) For additional, select examples of natural products that are apparently produced by Diels–Alder dimerization reactions, see the following. Absinthin: (a) Beauhaire, J.; Fourrey, J. L.; Vuilhorgne, M.; Lallemand, J. Y. *Tetrahedron Lett.* **1980**, *21*, 3191. Bistheonellasterone: (b) Kobayashi, M.; Kawazoe, K.; Katori, T.; Kitagawa, I. *Chem. Pharm. Bull.* **1992**, *40*, 1773. Longithorones: (c) Fu, X.; Hossain, M. B.; Schmitz, F. J.; van der Helm, D. *J. Org. Chem.* **1997**, *62*, 3810. (d) Layton, M. E.; Morales, C. A.; Shair, M. D. *J. Am. Chem. Soc.* **2002**, *124*, 773. Bisgersolanolide: (e) Rodriguez, A. D.; Shi, J.-G.; *Org. Lett.* **1999**, *1*, 337. (f) Nicolaou, K. C.; Vassilikogiannakis, G.; Simonsen, K. B.; Baran, P. S.; Zhong, Y.-L.; Vidali, V. P.; Pitsinos, E. N.; Couladouros, E. A. *J. Am. Chem. Soc.* **2000**, *122*, 3071 and references therein. (g) For a recent review of Diels–Alder type natural products, see: Ichihara, A.; Oikawa, H. *Curr. Org. Chem.* **1998**, *2*, 365.
- (10) Li, C.; Lobkovsky, E.; Porco, J. A., Jr. *J. Am. Chem. Soc.* **2000**, *122*, 10484.
- (11) In refs 8a and 10, epoxyquinol and epoxyquinone dimers were referred to as “*exo*”. However, it is more appropriate to refer to the dimers as “*endo*” with respect to the carbonyl substituent on the 2*H*-pyran dienophile.

[†] Boston University.

[‡] University of New Hampshire.

- (1) Presented in part at the 224th National Meeting of the American Chemical Society, Boston, MA, August 18–22, 2002; ORGN abstract 899.
- (2) (a) Strobel, G.; Yang, X.; Sears, J.; Kramer, R.; Sidhu, R. S.; Hess, W. M. *Microbiology* **1996**, *142*, 435. (b) Strobel, G. A. *Can. J. Plant Pathol.* **2003**, *24*, 14.
- (3) (a) Lee, J. C.; Yang, X.; Schwartz, M.; Strobel, G. A.; Clardy, J. *Chem. Biol.* **1995**, *2*, 721. (b) Lee, J. C.; Strobel, G. A.; Lobkovsky, E.; Clardy, J. *J. Org. Chem.* **1996**, *61*, 3232. (c) Jarvis, B. B. *Chemtracts: Org. Chem.* **1997**, *10*, 10.
- (4) Justman, C. J. Ph.D. Thesis, Harvard University, 2000. *Diss. Abstr. Int., B* **2000**, *61*, 2521.
- (5) Li, J. Y.; Harper, J. K.; Grant, D. M.; Tombe, B. O.; Bashyal, B.; Hess, W. M.; Strobel, G. A. *Phytochemistry* **2001**, *56*, 463.
- (6) Li, J. Y.; Strobel, G. A. *Phytochemistry* **2001**, *57*, 261.

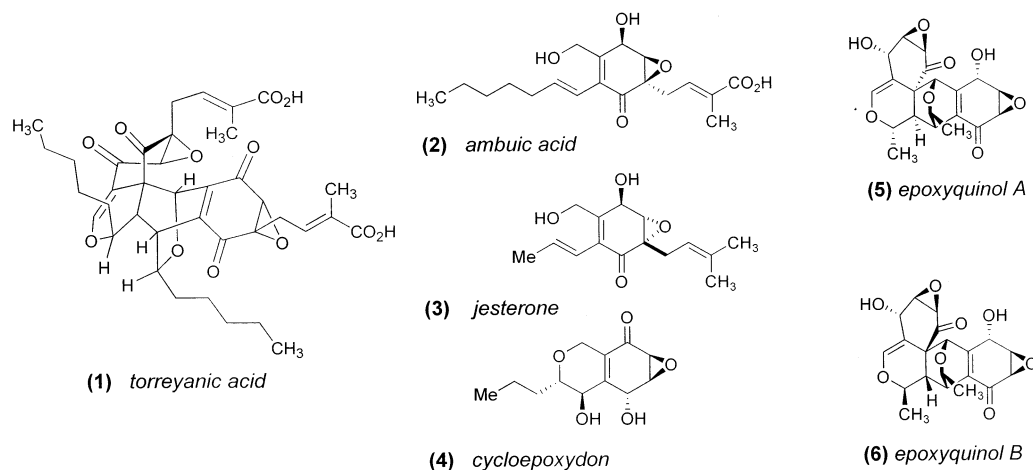


Figure 1. Torreyanic acid and related epoxyquinoid natural products.

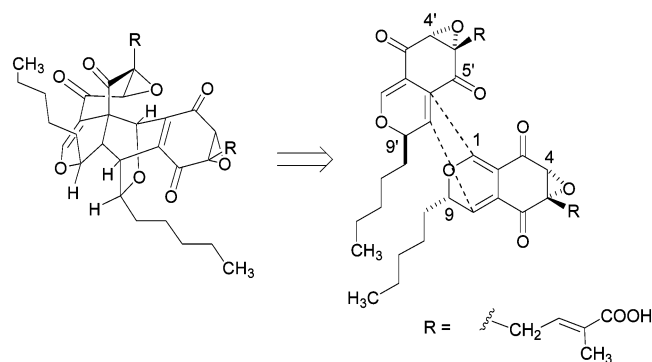


Figure 2. Proposed biosynthesis of torreyanic acid.

the Diels–Alder transition state. The isolation of the monomeric epoxyquinol, ambuic acid (**2**, Figure 1), from *P. microspora* further supports the proposed biosynthesis of torreyanic acid via oxidative dimerization of monomeric intermediates.

In a previous report,¹⁰ we described a synthesis of racemic torreyanic acid which demonstrated the feasibility of a biomimetic oxalelectrocyclization/Diels–Alder cascade. Herein, we report full account of the total synthesis and absolute stereochemical assignment of (+)-torreyanic acid. The asymmetric synthesis was facilitated by an adaptation of our recently developed method for tartrate-mediated nucleophilic epoxidation of quinone monoketals involving hydroxyl group direction.¹²

Synthetic Plan. A retrosynthetic analysis for the synthesis of torreyanic acid is depicted in Figure 3. Bis-*tert*-butyl ester **7** was chosen as the immediate precursor to **1** due to the reported stability of quinone epoxides to acidic conditions¹³ and general instability to basic conditions and nucleophiles.¹⁴ Compound **7** may be synthesized by oxidation/electrocyclization/Diels–Alder heterodimerization of diastereomeric *2H*-pyran monomers **8/8'**. Although *2H*-pyrans have been employed in intermolecular Diels–Alder reactions with reactive dienophiles,¹⁵ at the outset of our studies Diels–Alder dimerization of *2H*-pyran-4,5 diones had not been previously described. In this biomimetic, *endo*-selective Diels–Alder heterodimerization, the pentyl side chains

of the pyrans are *anti* to each other presumably to avoid severe steric interactions. Diastereomers **8/8'** may be derived from quinone monoepoxide **9** by oxidation, and *2H*-pyran formation, via 6π -electrocyclic ring-closure¹⁶ of the corresponding dienal **10**. Quinone monoepoxide **9** will be derived from quinone monoketal **11** by consecutive regio- and stereoselective epoxidation, transition-metal coupling¹⁷ of an *E*-vinyl stannane, followed by removal of protecting groups. The elaboration of the allyl group to a protected 2-methyl-2-butenic acid side chain may be achieved by alkene oxidation and Wittig olefination. Compound **11** could likewise be accessed by successive aromatic Claisen rearrangement and oxidation of aryl allyl ether **12**.

At the outset of our investigation, the factors involving formation and Diels–Alder dimerization of *2H*-pyrans such as **8/8'** were not entirely clear. Our approach to torreyanic acid (Figure 3) required valence isomerization of dienal **10** to *2H*-pyrans **8/8'**. The parent disrotatory cyclization of (*Z*)-2,4-pentadienal to *2H*-pyran has previously been studied at various levels of theory.¹⁸ Depending on the starting conformation, ring-closure is slightly endothermic, and the barrier is approximately 21–24 kcal/mol. This indicates a process that should easily proceed at ambient temperature. Figure 4 shows several literature examples delineating substituent effects on equilibria of dienal/dienone and *2H*-pyran valence isomers formed by 6π -electrocyclization.¹⁹ On the basis of these and related literature precedents, two generalizations may be formulated. First, increase in steric bulk shifts the equilibrium from the *cis*-dienal or dienone toward the *2H*-pyran (cf. **13** \rightarrow **14**^{20a} vs **15** \rightarrow **16**^{20b}). Second, the presence of electron-withdrawing groups, in particular at the 5-position of the *2H*-pyran, shifts the equilibrium toward the *2H*-pyran valence isomer (cf. **17** \rightarrow **18**^{20c} and **19** \rightarrow **20**^{20d}). These examples also gave us confidence that the equilibrium **10** \rightleftharpoons **8** (Figure 3) would lie to the right and favor

(12) Li, C.; Pace, E. A.; Liang, M.-C.; Lobkovsky, E.; Gilmore, T. D.; Porco, J. A., Jr. *J. Am. Chem. Soc.* **2001**, *123*, 11308.
 (13) (a) Ulrich, H.; Rao, D. V.; Tucker, B.; Sayigh, A. A. *R. J. Org. Chem.* **1974**, *39*, 2437. (b) Enhsen, A.; Karabelas, K.; Heerding, J. M.; Moore, H. W. *J. Org. Chem.* **1990**, *55*, 1177.
 (14) Genski, T.; Macdonald, G.; Wei, X.; Lewis, N.; Taylor, R. J. K. *Synlett* **1999**, 795.

(15) (a) Schiess, P.; Chia, H. L.; Suter, C. *Helv. Chim. Acta.* **1970**, *53*, 1713. (b) Royer, J.; Dreux, J. *Bull. Chim. Soc. Fr.* **1972**, 707. (c) Salomon, R. G.; Burns, J. R.; Dominic, W. *J. Org. Chem.* **1976**, *41*, 2918.
 (16) Krasnaya, Zh. A. *Chem. Heterocycl. Compd.* **2000**, *35*, 1255.
 (17) For a review of the Stille reaction, see: Farina, V.; Krishnamurthy, V.; Scott, W. *J. Org. React.* **1997**, *50*, 1.
 (18) Rodriguez-Otero, J. *J. Org. Chem.* **1999**, *64*, 6842.
 (19) For a discussion of substituent effects on equilibria between *2H*-pyrans and *cis*-dienones, see: Gosink, T. A. *J. Org. Chem.* **1974**, *39*, 1942.
 (20) (a) Blakemore, P. R.; Kocienski, P. J.; Marzcek, S.; Wicha, J. *Synthesis* **1999**, 1209. (b) Buchi, G.; Yang, N. C. *J. Am. Chem. Soc.* **1957**, *79*, 2318. (c) Ahluwalia, V. K.; Rao, J. S. *Indian J. Chem., Sect. B* **1989**, *28B*, 81. (d) Moorhoff, C. M. *Synthesis* **1987**, 685.

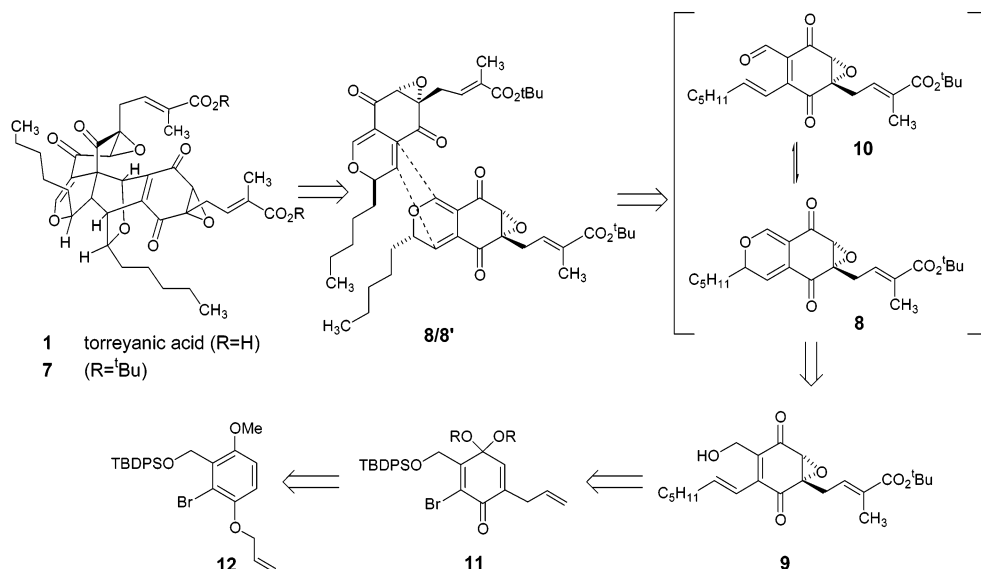


Figure 3. Retrosynthetic analysis.

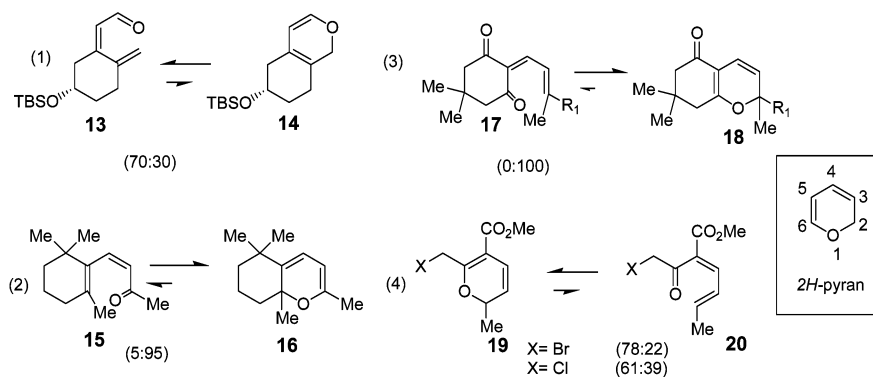
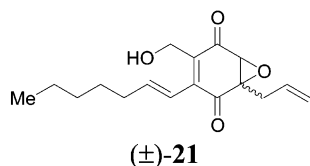


Figure 4. Dienal (dienone)/2H-pyran valence isomerization.

the 2H-pyran valence isomer. Second, successful production of torreyanic acid required an *endo*¹¹ Diels–Alder reaction, well-controlled diene facial selectivity, and an *anti* arrangement of the pentyl side chains. An intriguing aspect of the chemical synthesis of torreyanic acid was to determine whether diastereomeric products would be produced and further define the stereocontrol elements involved in the dimerization of these novel 2H-pyran-4,5 dione monomers.

Results and Discussion

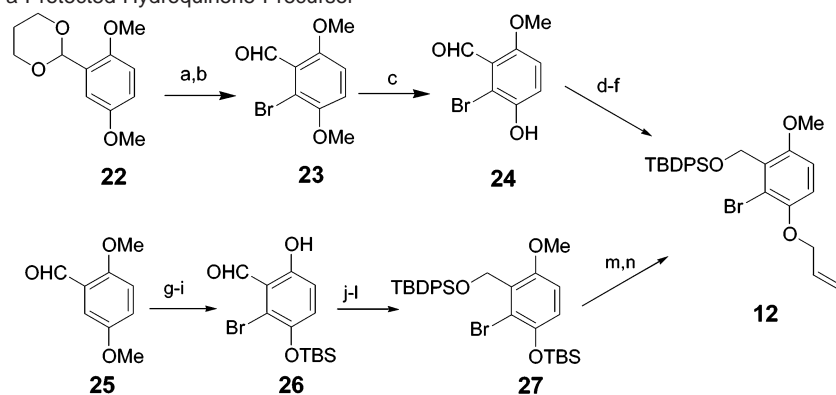
Synthesis of a Racemic, Model Substrate for Dimerization Studies. Our initial goal was to examine the synthesis and dimerization chemistry of a model 2H-pyran quinone epoxide substrate. Accordingly, we first targeted preparation of racemic quinone epoxide **21**. Studies were initiated to prepare aryl allyl



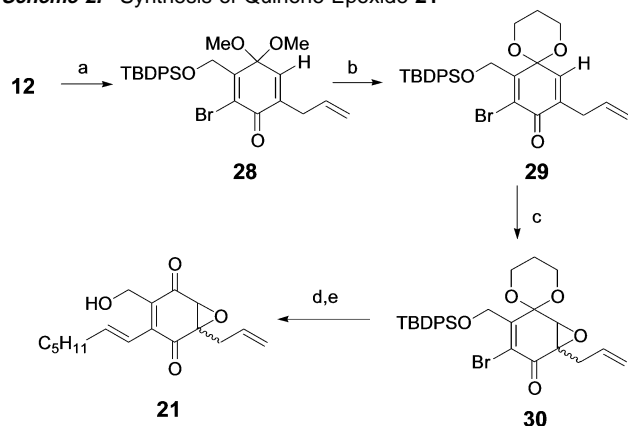
ether **12** which contains a protected hydroquinone precursor to a quinone monoketal, an aryl bromide for coupling to vinylmetal reagents, and a silyl-protected hydroxymethyl for use in 2H-

pyran formation. In our first-generation approach (Scheme 1),¹⁰ acetal **22** was converted to **23** by a cyclic acetal-directed lithiation–bromination protocol²¹ followed by acidic hydrolysis of the acetal. Regioselective demethylation²² of **23** afforded phenol **24**, which was converted to **12** by a reaction sequence of steps involving allylation, borohydride reduction, and silyl protection. Due to the difficulty in performing large-scale lithiation reactions and moderate yields obtained in the selective demethylation of **23**, we subsequently developed a second-generation synthesis of aromatic precursor **12**.²³ The latter synthesis began with commercially available 2,5-dimethoxy benzaldehyde, **25**. Demethylation of **25** with boron tribromide (2.5 equiv) followed by regioselective bromination²⁴ and selective silylation²⁵ (TBSCl, imidazole) provided phenol **26**. Methylation of **26**, followed by reduction and protection of the derived alcohol with TBDPSCI, afforded bis-silyl ether **27**. After

- (21) For directed ortho-lithiation of aromatic acetals, see: (a) Plaumann, H. P.; Keay, B. A.; Rodrigo, R. *Tetrahedron Lett.* **1979**, *20*, 4921. (b) Costa, P. R. R.; Lopes, C. C.; Lopes, R. S. C.; Marinho, M. F. G.; Castro, R. N. *Synth. Commun.* **1988**, *18*, 1723.
- (22) Ulrich, H.; Rao, D. V.; Tucher, B.; Sayigh, A. A. R. *J. Org. Chem.* **1974**, *39*, 2437.
- (23) Hu, Y.; Li, C.; Kulkarni, B.; Strobel, G.; Lobkovsky, E.; Torczynski, R. M.; Porco, J. A., Jr. *Org. Lett.* **2001**, *3*, 1649.
- (24) Narayanan, V. L.; Sausville, E. A.; Kaur, G.; Varma, R. K. PCT Int. Appl. WO 9943636, 1999.
- (25) For example, see: Liu, A.; Dillon, K.; Campbell, R. M.; Cox, D. C.; Hurn, D. M. *Tetrahedron Lett.* **1996**, *37*, 3785.

Scheme 1. Syntheses of a Protected Hydroquinone Precursor^a

^a Reagents and conditions: (a) (i) BuLi, 3:1 hexane/benzene, $-25\text{ }^{\circ}\text{C}$, 10 h, (ii) $\text{BrCF}_2\text{CF}_2\text{Br}$, THF, 0.5 h, 70%; (b) 11 M HCl, THF, 10 min, 100%; (c) H_2SO_4 , $70\text{ }^{\circ}\text{C}$, 14 h, 52%; (d) allyl bromide, K_2CO_3 , DMF, 3 h; (e) NaBH_4 , EtOH, 0.5 h; (f) TBDPSCI, imid., DMF, 2.5 h (90% for three steps); (g) BBr_3 , CH_2Cl_2 , $-78 \rightarrow 0\text{ }^{\circ}\text{C}$, 1 h, 97%; (h) Br_2 , CHCl_3 , rt, 2.5 h, 94%; (i) TBDMSCl, imidazole, CH_2Cl_2 , rt, 20 min, 94%; (j) MeI, NaH, THF, $65\text{ }^{\circ}\text{C}$, 7 h, 72%; (k) NaBH_4 , EtOH, $0\text{ }^{\circ}\text{C}$, 0.5 h, 100%; (l) TBDPSCI, imidazole, DMF, rt, 6 h, 93%; (m) TBAF, THF, $0\text{ }^{\circ}\text{C}$, 5 min, 100%; (n) allyl bromide, K_2CO_3 , DMF, 3 h, 97%.

Scheme 2. Synthesis of Quinone Epoxide **21**^a

^a Reagents and conditions: (a) (i) neat, $180\text{ }^{\circ}\text{C}$, 2 h (ii) $\text{PhI}(\text{OAc})_2$, MeOH, 20 min; 70%; (b) $\text{HO}(\text{CH}_2)_3\text{OH}$, PPTS, benzene, $80\text{ }^{\circ}\text{C}$, 20 min, 90%; (c) Ph_3COOH , KHMDS, THF, $-78 \rightarrow -20\text{ }^{\circ}\text{C}$, 6 h, 81%; (d) (*E*)-tributyl-1-heptenyl-stannane, $\text{Pd}(\text{PPh}_3)_4$, PhCH_3 , $110\text{ }^{\circ}\text{C}$, 4 h, 98%; (e) 48% aq HF, CH_3CN , 7 h, 76%.

selective deprotection of **27** (TBAF), the resulting phenol was allylated to afford the desired phenyl allyl ether **12** (10–20 g scale).

Thermolysis of **12** (neat) led to facile aromatic Claisen rearrangement to afford an ortho-allylated phenol, which was directly oxidized²⁶ to dimethoxyketal **28** (Scheme 2). On the basis of the well-described use of quinone monoacetals as substrates for nucleophilic epoxidation,²⁷ we proceeded with evaluation of substrate **28**. However, dimethoxyacetal **28** was found to be essentially unreactive to nucleophilic epoxidation conditions known to effect monoepoxidation of quinone monoketals or quinones (e.g., $^t\text{BuOOH}$ (DBU,^{28a} TBD,¹⁴ or BuLi ^{28b}), $\text{H}_2\text{O}_2/\text{K}_2\text{CO}_3$, $\text{NaBO}_3/\text{aq EtOH}$,^{28c} and cumene hydroperoxide/ NaH ^{28d}). After considerable experimentation, we found that

epoxidation of **28** with Ph_3COOH ²⁹ (KHMDS, $-78 \rightarrow -35\text{ }^{\circ}\text{C}$, 72 h) led to approximately 20% conversion to a monoepoxide product. However, acetal exchange of **28** with 1,3-propanediol afforded 1,3-dioxane **29** which was smoothly epoxidized to afford monoepoxide **30** (81%). Attachment of the alkenyl side chain was accomplished by Stille coupling¹⁷ with (*E*)-tributyl-1-heptenyl stannane. Exposure of the diene intermediate to aqueous HF/ CH_3CN effected sequential hydrolysis of cyclic acetal and silyl ether protecting groups to afford the target quinone epoxide **21**. It should be noted that the additional conjugation afforded by the α -heptenyl enone facilitated rapid (5 min) acetal hydrolysis to the quinone monoepoxide. Hydrolysis of bromo-acetal **30** using identical conditions (48% aqueous HF/ CH_3CN) provided the corresponding quinone epoxide less efficiently (acetal hydrolysis incomplete after 2 h).

To understand the difference in epoxidation reactivity of dimethoxyketal **28** and cyclic ketal **29**, we first compared their ^1H and ^{13}C NMR spectra. Examination of the ^1H NMR resonance for C5–H in **29** showed a downfield shift of 0.83 ppm relative to **28** and a 7.0 ppm upfield shift of C5 in the ^{13}C NMR spectrum (Figure 5). To further understand the relative NMR chemical shifts as well as the reactivity differences, single-crystal X-ray structures of **28** and **29** were obtained (Figure 5). The X-ray structures show that cyclic ketal **29** adopts chair conformation **A** instead of **B** to avoid severe steric interactions between the indicated methylene hydrogens and the allylic silyl ether.²³ In this X-ray structure, the two axial hydrogens of the cyclic ketal show close contact with the C5 vinylic hydrogen (2.20–2.21 Å). It has been demonstrated that nonbonded repulsions between proximate hydrogens can cause an increase in shielding experienced by the associated ^{13}C nuclei³⁰ (γ -gauche interaction³¹), as well as lower-field proton chemical shifts due to sterically induced charge polarization by H–H repulsion.³² The NMR chemical shift differences observed in **28** and **29** may

(26) (a) Pelter, A.; Elgandy, S. *Tetrahedron Lett.* **1988**, *29*, 677. (b) Fleck, A. E.; Hobart, J. A.; Morrow, G. W. *Synth. Commun.* **1992**, *22*, 179.

(27) (a) Wipf, P.; Kim, Y. *J. Org. Chem.* **1994**, *59*, 3518. (b) Wipf, P.; Kim, Y.; Jahn, H. *Synthesis* **1995**, *12*, 1549. (c) Wipf, P.; Coish, P. D. *J. Org. Chem.* **1999**, *64*, 5053. (d) Alcaraz, L.; Macdonald, G.; Ragot, J. P.; Taylor, R. J. K.; Alcaraz, L.; Kapfer-Eyer, I.; Macdonald, G.; Wei, X.; Lewis, N. *Synthesis* **1998**, *15*, 775. (e) Alcaraz, L.; Macdonald, G.; Ragot, J. P.; Lewis, N.; Taylor, R. J. K. *J. Org. Chem.* **1998**, *63*, 3526. (f) Alcaraz, L.; Macdonald, G.; Ragot, J.; Lewis, N. *J. Tetrahedron* **1999**, *55*, 3707. (g) Cronje Grove, J. J.; Wei, X.; Taylor, R. J. K. *Chem. Commun.* **1999**, *5*, 421.

(28) (a) Schlessinger, R. H.; Beberitz, G. R.; Lin, P. *J. Am. Chem. Soc.* **1985**, *107*, 1777. (b) Meth-Cohn, O.; Moore, C.; Taljaard, H. C. *J. Chem. Soc., Perkin. Trans.* **1988**, 2663. (c) Ichihara, A.; Oda, K.; Sakamura, S. *Tetrahedron Lett.* **1972**, *50*, 5105. (d) Wipf, P.; Jung, J.-K. *J. Org. Chem.* **1998**, *63*, 3531.

(29) Corey, E. J.; Wu, L. I. *J. Am. Chem. Soc.* **1993**, *115*, 9327.

(30) Grant, D. M.; Cheney, B. V. *J. Am. Chem. Soc.* **1967**, *89*, 5315.

(31) Also known as the γ effect, see: (a) Dalling, D. K.; Grant, D. M. *J. Am. Chem. Soc.* **1972**, *94*, 5318. (b) Smith, D. H.; Jurs, P. C. *J. Am. Chem. Soc.* **1978**, *100*, 3316.

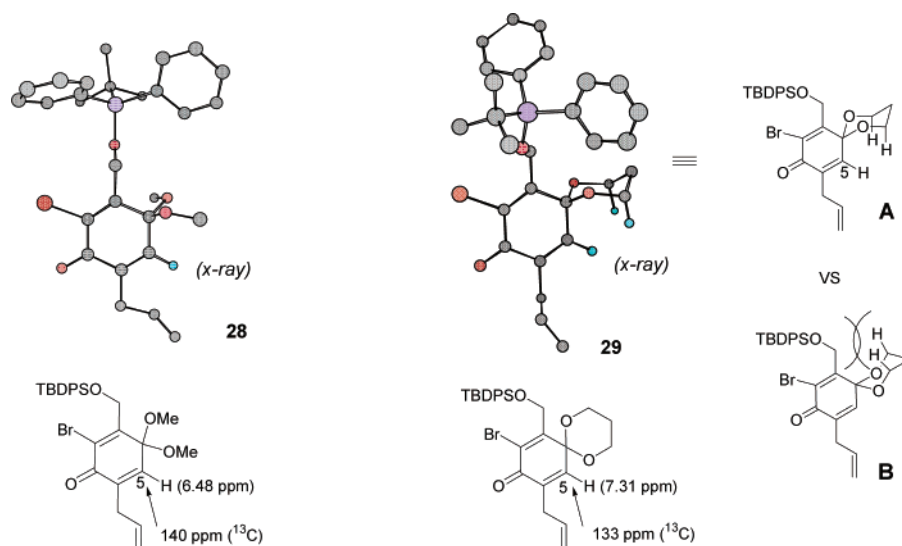
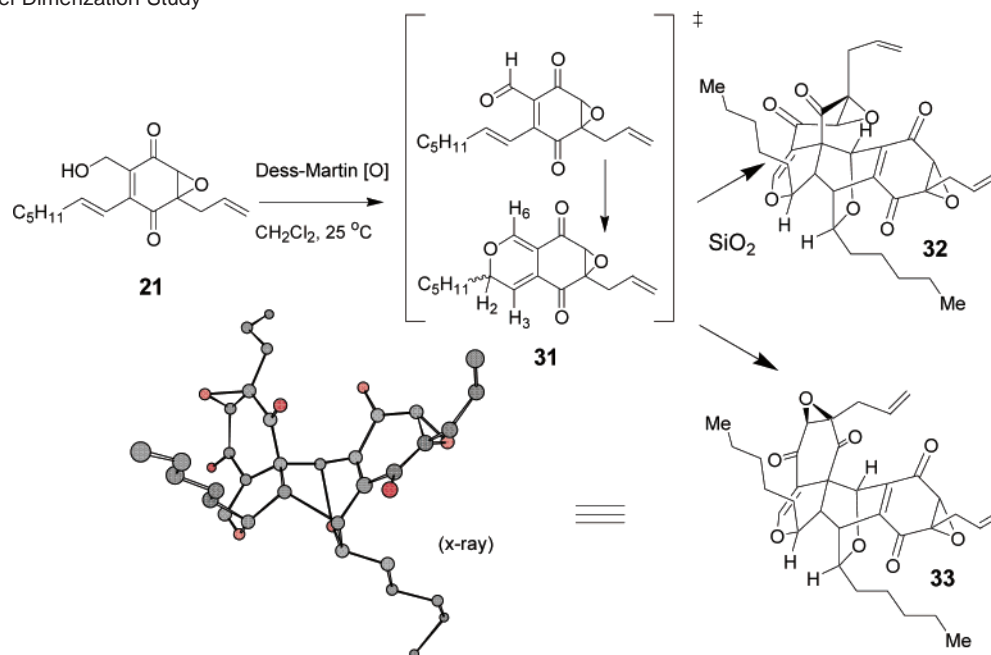


Figure 5. X-ray crystal structures of acyclic and cyclic quinone monoketals.

Scheme 3. Model Dimerization Study



thus be explained by the X-ray structure but are not necessarily correlated with the epoxidation reactivity of these substrates. However, further comparison of the X-ray structures provides additional clues about the epoxidation reactivity. As shown in the X-ray structure of **29**, the fixed 1,3-dioxane chair conformation may minimize electrostatic repulsion between the oxygen lone pairs and the incoming electron-rich peroxide.³³ Moreover, free rotation of methoxy groups in **28** may disturb 1,4-addition of the approaching peroxide anion, which is the rate-determining step for nucleophilic epoxidation.³⁴

Feasibility Study for Diels–Alder Dimerization. A model study for the tandem oxidation/ 6π -electrocyclization/dimerization process was next undertaken. Gratifyingly, treatment of

racemic quinone epoxide **21** with Dess–Martin periodinane afforded a crude mixture of 2*H*-pyran **31** (approximately 1:1 mixture of diastereomers) and two dimeric products (monomers: dimers approximately 2.6:1) (Scheme 3). After silica gel chromatography, only dimeric products **32** (26%) and **33** (46%) were isolated, indicating acid catalysis of the dimerization. In practice, following oxidation the reaction mixture was allowed to stand on a silica gel column for 1 h to effect complete Diels–Alder dimerization prior to elution of products.³⁵ Similarly, incubation of the crude oxidation reaction mixture with the mildly Lewis acidic clay, Montmorillonite K10 (CH_2Cl_2), was found to afford dimeric products.³⁶ The major dimeric product

(32) Cheney, B. V. *J. Am. Chem. Soc.* **1968**, *90*, 5386.

(33) For an example of nucleophilic addition *anti* to an alkoxy group due to apparent repulsive interactions, see: Smith, A. B., III; Dunlap, N. K.; Sulikowski, G. A. *Tetrahedron Lett.* **1988**, *29*, 439.

(34) Bunton, C. A.; Minkoff, G. J. *J. Chem. Soc.* **1949**, 665.

(35) For recent examples of Diels–Alder reactions catalyzed by silica gel, see: 1. (a) Leon, F. M.; Carretero, J. C. *Tetrahedron Lett.* **1991**, *32*, 5405. (b) Wang, W. B.; Roskamp, Eric J. *Tetrahedron Lett.* **1992**, *33*, 763. (c) Posner, G. H.; Carry, J. C.; Lee, J. K.; Bull, D. S.; Dai, H. *Tetrahedron Lett.* **1994**, *35*, 132. (d) Cativiela, C.; Garcia, J. I.; Mayoral, J. A.; Pires, E.; Royo, A. J.; Figueras, F. *Tetrahedron* **1995**, *51*, 1295. (e) Perez, J. M.; Lopez-Alvarado, P.; Alonso, M. A.; Avendano, C.; Menendez, J. Carlos. *Tetrahedron Lett.* **1996**, *37*, 6955.

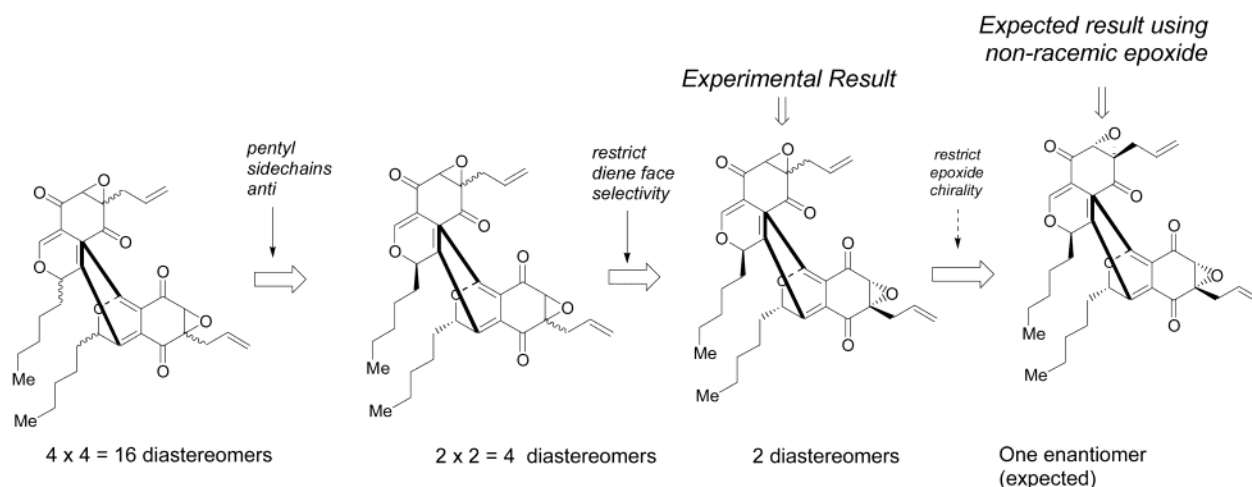


Figure 6. Apparent stereocontrol elements in Diels–Alder dimerization of 2*H*-pyran quinone epoxide monomers.

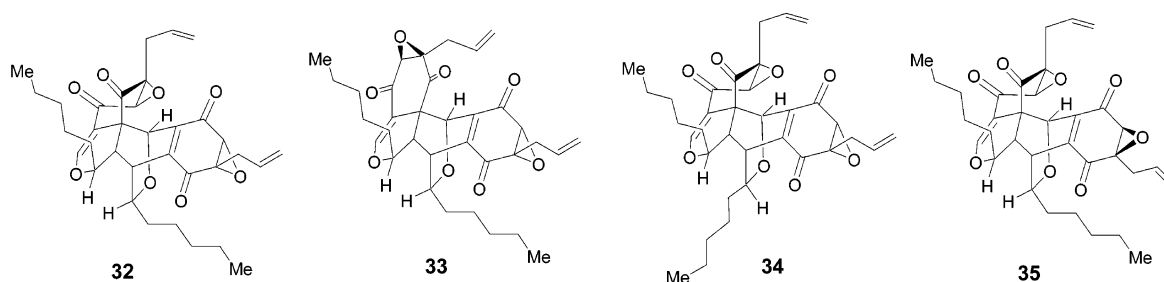


Figure 7. Chemical Structures used for transition-state energy calculation.

33 was produced by *endo*-selective Diels–Alder dimerization of heterochiral 2*H*-pyran epoxides as determined by single-crystal X-ray structure analysis. The structure of the minor dimer **32** was assigned as the torreyanic acid core structure by comparison to the ^1H NMR spectrum of the natural product and subsequent preparation of torreyanic acid. It should be noted that both **32** and **33** are produced from Diels–Alder dimerization reactions in which the pentyl side chains are *anti* to one another in the [4 + 2] transition state and the dienophile approaches the diene *anti* to the epoxide moiety.³⁷

These initial model studies in the racemic series provided insight into the stereocontrol elements involved in the dimerization of 2*H*-pyran-4,5 dione monomers produced by tandem oxidation/electrocyclization. As illustrated in Figure 6, if we restrict the Diels–Alder dimerization reaction to be *endo*- and regioselective, $4 \times 4 = 16$ possible diastereomers may be produced. An additional set of 16 enantiomers of these structures may be produced by altering the facial selectivity of the diene and dienophile. Our experimental results thus far may be explained by restrictions imposed by a series of apparent stereocontrol elements (Figure 6). First, *anti* orientation of the pentyl side chains reduces the total number of diastereomers from sixteen to four. Second, Diels–Alder cycloaddition in which the diene face selectivity is *anti* to the epoxide³⁷ further reduces the number of possibilities to two diastereomers, which is observed experimentally (four enantiomers). Utilization of a nonracemic sample of the epoxide monomer is expected to produce a single enantiomer of torreyanic acid, which will be discussed in a later section regarding asymmetric synthesis. From the aforementioned analysis one important conclusion can be made: by employing a nonracemic epoxide, it is possible to generate either enantiomer of compound **32** to the exclusion of the

heterochiral dimer **33**. However, **33** can only be prepared as a racemate since it arises by dimerization of a pair of enantiomers.

Transition-State Analysis of Model Dimerization. To further understand the Diels–Alder dimerization results observed by experiments, we carried out theoretical calculations³⁸ of Diels–Alder transition states.³⁹ The torreyanic acid structure was first simplified to an allyl side chain (cf. Scheme 3, **32**), for which we have experimental results. For illustration of the two stereocontrol elements (pentyl side chain and epoxide of the diene), we compared transition-state energies of structures **32**–**35** (Figure 7). In structure **34**, the pentyl side chain of the diene is *syn* to the approaching dienophile. In structure **35**, the epoxide of the diene is *syn* to the approaching dienophile.

To rapidly locate the numerous minima and transition states on this complex potential energy surface, we chose a hybrid theoretical method. All structures were optimized and

- (36) For select examples of Diels–Alder reactions catalyzed by montmorillonite K10 clay, see: (a) Laszlo, P.; Lucchetti, J. *Tetrahedron Lett.* **1984**, 25, 2147. (b) Cativiela, C.; Figueras, F.; Fraile, J. M.; Garcia, J. I.; Mayoral, J. A. *Tetrahedron: Asymmetry* **1993**, 4, 223. (c) Chiba, K.; Hirano, T.; Kitano, Y.; Tada, M. *Chem. Commun.* **1999**, 8, 691. (d) Kamath, C. R.; Samant, S. D. *Indian J. Chem., Sect. B* **1999**, 38B, 1214. (e) For a review of recent advances in clay-catalyzed organic transformations, see: Nikalje, M. D.; Phukan, P.; Sudalai, A. *Org. Prep. Proced. Int.* **2000**, 32, 1.
- (37) For an example of Diels–Alder cycloaddition with π -facial selectivity *anti* to the diene epoxide moiety, see: J. R. Gillard, M. J. Newlands, J. N. Bridson, D. J. Burnell, *Can. J. Chem.* **1991**, 69, 1337.
- (38) All calculations were performed using Spartan 02 (Version 1.01, Wavefunction, Inc., Irvine, CA.).
- (39) For recent theoretical calculations of Diels–Alder transition states, see: (a) Ujaque, G.; Norton, J. E.; Houk, K. N. *J. Org. Chem.* **2002**, 67, 7179. (b) Cayzer, T. N.; Wong, L. S.-M.; Turner, P.; Paddon-Row: M. N.; Sherburn, M. S. *Chem. Eur. J.* **2002**, 8, 739. (c) Singleton, D. A.; Schulmeier, B. E.; Hang, C.; Thomas, A.; Leung, S.-W.; Merrigan, S. R. *Tetrahedron* **2001**, 57, 5149. (d) Paddon-Row: M. N.; Sherburn, M. S. *Chem. Commun.* **2000**, 22, 2215 (e) Bachmann, C.; Boeker, N.; Mondon, M.; Gesson, J.-P. *J. Org. Chem.* **2000**, 65, 8089. (f) Bradley, A. Z.; Kociolk, M. G.; Johnson, R. P. *J. Org. Chem.* **2000**, 65, 7134.

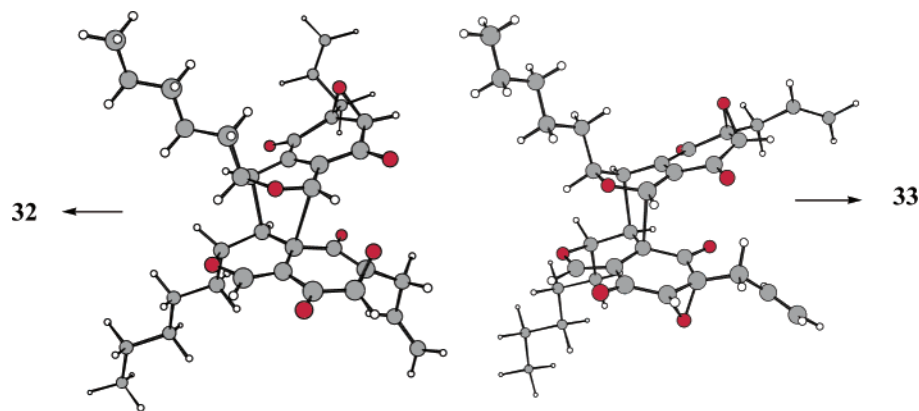


Figure 8. Model transition states leading to **32** and **33**.

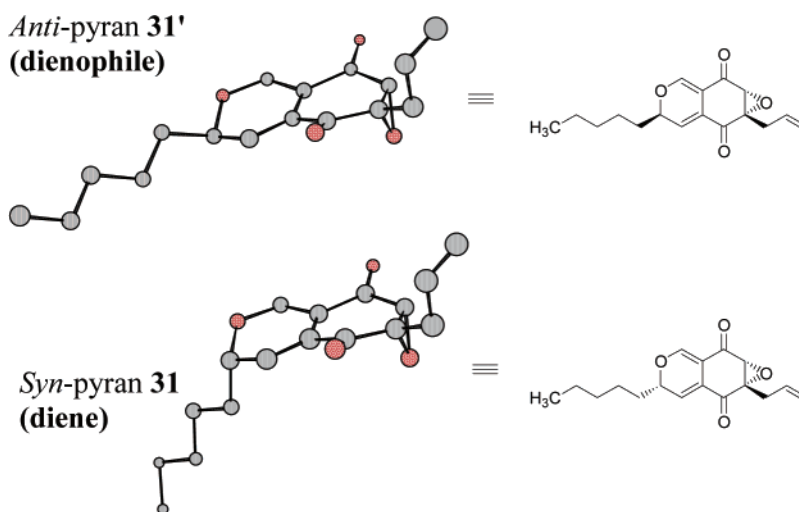


Figure 9. Optimized geometries for the pyrans.

subjected to frequency analysis with the semiempirical AM1 method, followed by a single-point B3LYP/6-31G* calculation. AM1 zero-point corrections were then applied to arrive at a final relative energy.⁴⁰ Transition-state models were initially constructed with the pentyl side chain in the most extended conformation. Other conformations are possible but should not significantly change the energetics.

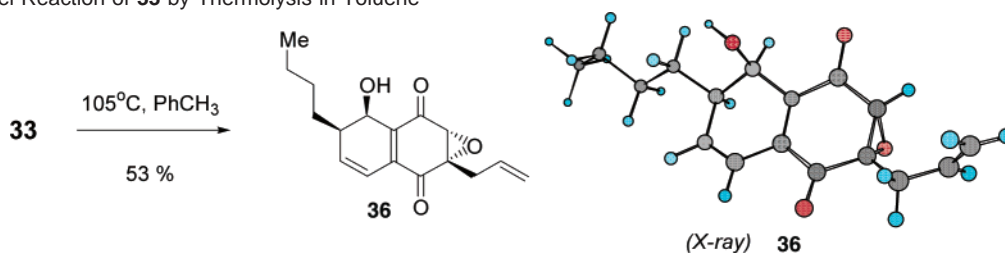
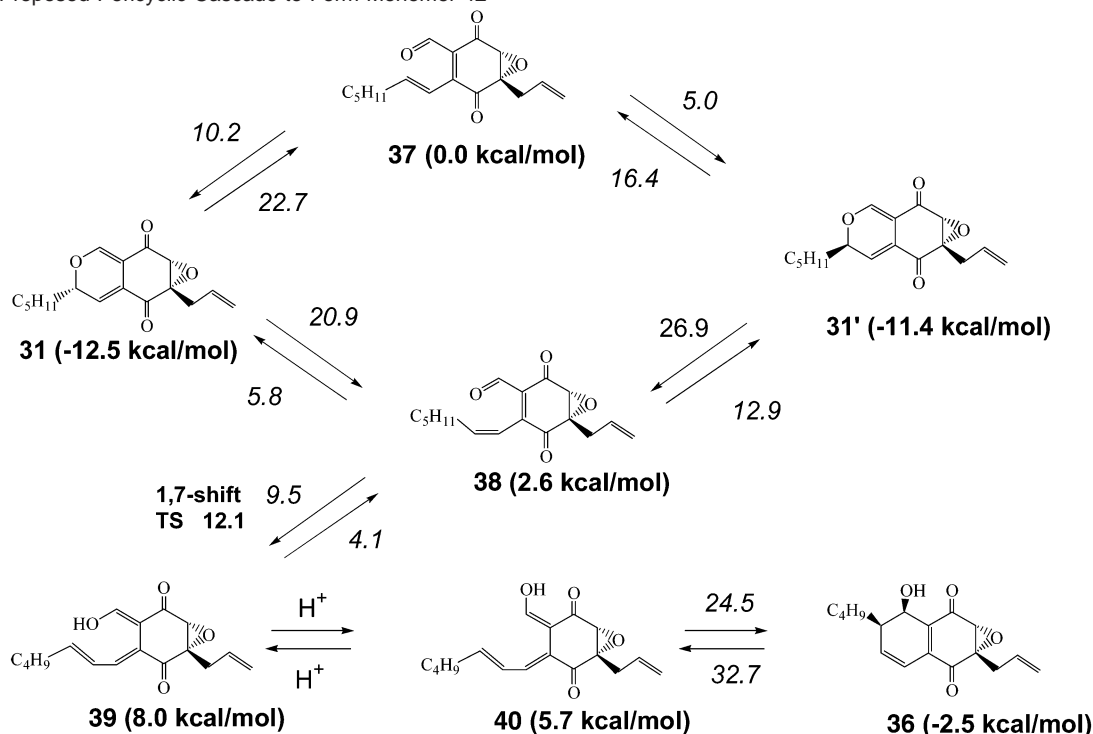
At the B3LYP//AM1 level of theory, transition states leading to **32**, **33**, **34**, and **35** were predicted to be 18.5, 20.0, 27.9, and 31.6 kcal/mol above reactants, respectively. Other selected regio- and stereochemical modes of addition were investigated; all gave predicted barriers of >25 kcal/mol. We conclude from these studies that the lowest-energy [4 + 2] transition state leads to **32**, which resembles the torreyanic acid core structure. In contrast, dimerization of a racemic mixture **31** affords a second energetically competitive transition state, which leads to dimer **33**. Transition-state structures leading to diastereomers **32** and **33** are shown in Figure 8. These computational results are consistent with our experiments on racemic and enantiomerically pure material (see later section regarding asymmetric synthesis

of (+)-torreyanic acid). Lewis acid catalysis is also possible, but we have not carried out calculations on this process.

Figure 9 shows the B3LYP/6-31G* optimized structures (hydrogens omitted for clarity) for the diastereomeric pyrans **31** and **31'**. In each case, only one ring conformer could be located. For *anti*-pyran **31'**, the pentyl side chain adopts an equatorial orientation, while for the *syn*-pyran **31**, the pentyl side chain adopts an axial orientation, which leaves the other face (also *anti* to epoxide) open to the dienophile. These conformations suggest that only the *syn*-pyran may serve as a diene because it has a more sterically accessible face (*anti* to the epoxide) for an incoming dienophile, which is consistent with our experimental results. Thus, the orientation of the pentyl groups in the lower-energy transition states may largely be controlled by steric factors. Analysis of the frontier molecular orbitals revealed no obvious basis for facial selectivity. The observed regio- and stereochemistry of cycloaddition can be explained by a conventional frontier MO analysis, which pairs the diene HOMO with the dienophile LUMO. Symmetry-favorable secondary interactions further support the *endo* orientation. The same is true for the complementary LUMO–HOMO pair of orbitals.

The Diels–Alder cycloaddition normally is exothermic by approximately 30–40 kcal/mol.⁴¹ In the present case, structural congestion in the product is expected to diminish this value significantly. At the B3LYP//AM1 level, the predicted energy

(40) This method is denoted as B3LYP/6-31G**/AM1(+ZPVE). Selected DFT optimizations were carried out to validate this method. For example, the barrier to closure for the *trans*-dienal to *syn*-pyran **31** (epoxide and pentyl chain *syn* refer to the pyran-fused quinone plane) was calculated to be 10.2 kcal/mol at the DFT//AM1 level and 12.6 kcal/mol with B3LYP/6-31G* theory. The parent dienal cyclization has a predicted barrier of ca. 22 kcal/mol, see ref 18.

Scheme 4. Novel Reaction of **33** by Thermolysis in Toluene**Scheme 5.** Proposed Pericyclic Cascade to Form Monomer **42^a**

^a Barriers (italics) and energetics (boldface in brackets).

change upon formation of **32** and **33** by cycloaddition is -8.0 and -5.3 kcal/mol, respectively. These modest exothermicities suggest facile reversibility in the cycloaddition reactions (vide infra).

Thermolysis Studies of Quinone Epoxide Dimers. Given the moderate calculated exothermicities of *2H*-pyran dimerizations (vide supra), we reasoned that retro Diels–Alder reaction of the dimers should occur under thermolytic conditions. Thermolysis of dimer **33** was first conducted at 105 °C (toluene, 9 h) in which case a novel monomeric compound (**36**) was formed in 53% yield (Scheme 4). The relative configuration of the stereocenters in **36** was determined by single-crystal X-ray structure analysis.

Scheme 5 presents a proposed mechanism⁴² for formation of **36**, including a summary of proposed intermediates and energetics calculated using the B3LYP//AM1 method. *trans*-Dienal **37** is the experimental starting point and energetic reference. Numbers indicated above the arrows represent barriers (kcal/

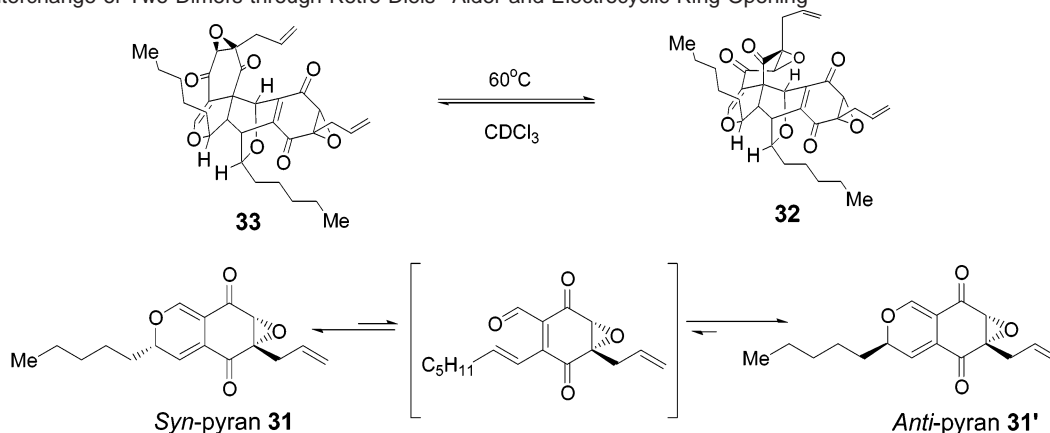
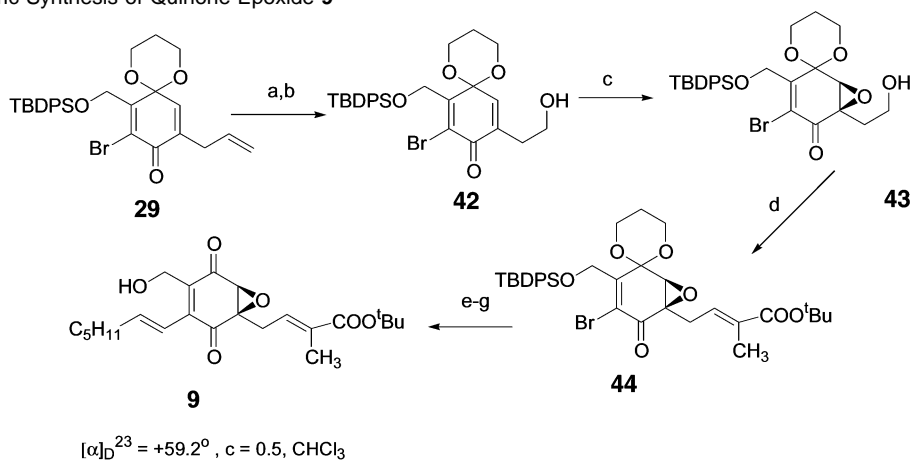
mol) in each direction. Two low-energy, disrotatory pathways exist for cyclization to diastereomeric *syn* or *anti* *2H*-pyrans **31** or **31'**. The predicted barriers are consistent with the facile electrocyclicization we observe experimentally. Two additional disrotatory paths connect the pyrans with *cis*-dienal **38**. The *cis*-dienal then presents a favorable geometry for subsequent antarafacial 1,7-hydrogen migration⁴³ to trienol **39**, which then isomerizes to the lower-energy hydrogen-bonded stereoisomer **40**, presumably by trace-acid catalysis. The final step may be disrotatory cyclization to **36**. This final step should not be easily reversible because **36** lies in the deepest energy well on the surface. On the basis of this general mechanism, **36** should also be produced by **32**. In the event, thermolysis of **32** at 110 °C also produces monomeric compound **36** in 38% yield.

Since the aforementioned mechanism is initiated by a facile retro Diels–Alder reaction, we reasoned that thermolysis at lower temperature may prevent generation of **36** and lead to equilibration between two dimers **32** and **33**. In the event, simple

(41) On the basis of heats of formation, the parent [4 + 2] reaction is exothermic by 40 kcal/mol which is reduced in bicyclic structures, cf.: Wilsey, S.; Houk, K. N.; Zewail, A. H. *J. Am. Chem. Soc.* **1999**, *121*, 5772.

(42) Another possible mechanism for the production of alcohol **36** involves an ene reaction of **38** leading to a vinyl cyclobutene intermediate that either opens to **39** or **40**, or undergoes a vinyl cyclobutane rearrangement directly to **36**. We thank a reviewer for pointing out this possibility.

(43) The geometric requirements for antarafacial [1,7] sigmatropic shifts are well-known, see: (a) Jiao, H.; Schleyer, P. v. R. *Angew. Chem., Int. Ed. Engl.* **1993**, *32*, 1763. (b) Enas, J. D.; Shen, G. Y.; Okamura, W. H. *J. Am. Chem. Soc.* **1991**, *113*, 3873. (c) Shimizu, M.; Iwasaki, Y.; Ohno, A.; Yamada, S. *Chem. Pharm. Bull.* **2000**, *48*, 1484. (d) Millar, J. G. *Tetrahedron Lett.* **1997**, *38*, 7971. (e) Daniel, D.; Middleton, R.; Henry, H. L.; Okamura, W. H. *J. Org. Chem.* **1996**, *61*, 5617. (f) Pohnert, G.; Boland, W. *Tetrahedron* **1994**, *50*, 10235.

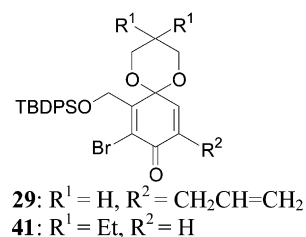
Scheme 6. Interchange of Two Dimers through Retro Diels–Alder and Electrocyclic Ring-Opening**Scheme 7.** Asymmetric Synthesis of Quinone Epoxide **9**^a

^a Reagents and conditions: (a) $\text{NaIO}_4, \text{OsO}_4, \text{THF}/\text{H}_2\text{O}$, 1.5 h, 62%; (b) $\text{BH}_3 \cdot \text{tBuNH}_2, \text{MeOH}/\text{H}_2\text{O}, \text{THF}$, 0 °C, 20 min, 76%; (c) $\text{Ph}_3\text{COOH}, \text{NaHMDS}, L\text{-DIPT}, 4 \text{ \AA MS}, \text{PhCH}_3, -40 \text{ }^\circ\text{C}$, 50 h, 91%, 91% ee; (d) (i) Dess–Martin periodinane, CH_2Cl_2 , 35 min (ii) $\text{PPh}_3=\text{C}(\text{CH}_3)\text{COOtBu}, \text{CH}_2\text{Cl}_2, -78 \rightarrow -5 \text{ }^\circ\text{C}$, 4 h, 94%; (e) (*E*)-tributyl-1-heptenylstannane, $\text{Pd}(\text{PPh}_3)_4, \text{PhCH}_3, 110 \text{ }^\circ\text{C}$, 2 h, 94%; (f) TBAF/AcOH (1:1), THF , 20 h, 76%; (g) 48% aq $\text{HF}, \text{CH}_3\text{CN}$, 15 min, 93%.

heating of dimer **33** (0.004 M, CDCl_3 , 60 °C) was found to be effective. After 1 h, NMR analysis showed the appearance of 2*H*-pyran monomers. Interestingly, after 24 h, dimer **32** was the major compound by NMR analysis. After 2 days, dimer **32** was isolated as the major product in 38% yield after silica gel chromatography. A parallel experiment showed that **33** is also formed by thermolysis of **32**. NMR integration showed that the equilibrium ratio of **31/31':32:33** (60 °C, 48 h in CDCl_3) was 5:4:1. Since the two pyrans of **33** are both *syn* and **32** is comprised of one *syn*- and one *anti*-pyran, it is apparent that this equilibration may occur through a process involving retro Diels–Alder reaction followed by electrocyclic ring-opening of the 2*H*-pyran (Scheme 6). No aldehyde proton signals were observed in the proton NMR spectra, which is related to the observation that no aldehyde peak was observed in the crude ^1H NMR spectrum after Dess–Martin oxidation (cf. Scheme 3). This reinforces the favorable equilibrium of the 2*H*-pyran valence isomer relative to the dienal form.

Asymmetric Syntheses of (+)-Torreyanic Acid and (+)-Ambuic Acid. In our racemic synthesis of model compound **21**, a nonstereoselective epoxidation was conducted on quinone monoketal **29**. We sought to develop reagent-controlled asymmetric nucleophilic epoxidation⁴⁴ of **29** to establish an asymmetric synthesis of torreyanic acid. We first studied the reactivity of substrate **29**, which bears an additional α -allyl substituent

relative to a workable substrate **41**, using our recently developed tartrate-mediated nucleophilic epoxidation method.¹² However,

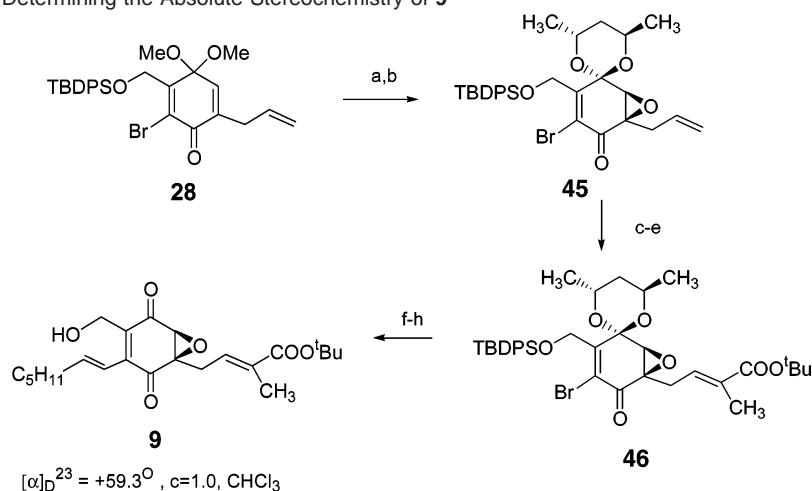


29 gave very low reactivity (rt, 20 h, <40% conversion) and afforded virtually no enantioselectivity (<10% ee). We decided to modify **29** to homoallylic alcohol **42** with the hope that the hydroxyl group could facilitate the epoxidation by directing group effects (Scheme 7).⁴⁵ The desired substrate **42** was prepared by Lemieux–Johnson oxidation of **29** and selective reduction of the aldehyde in the presence of the dienone ($\text{BH}_3 \cdot \text{tBuNH}_2$).⁴⁶ Gratifyingly, by using the tartrate-mediated

(44) For a recent review of asymmetric epoxidation of electron-deficient olefins, see: Porter, M. J.; Skidmore, J. *Chem. Commun.* **2000**, 14, 1215.

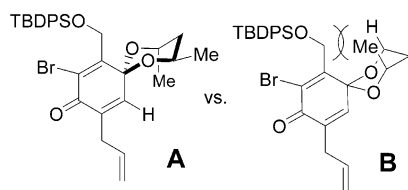
(45) For recent example of hydroxyl-directed nucleophilic epoxidation of an enone, see: Evarts, J. B., Jr.; Fuchs, P. L. *Tetrahedron Lett.* **1999**, 40, 2703.

(46) Andrews, G. C. *Tetrahedron Lett.* **1980**, 21, 697.

Scheme 8. Correlation for Determining the Absolute Stereochemistry of **9**^a

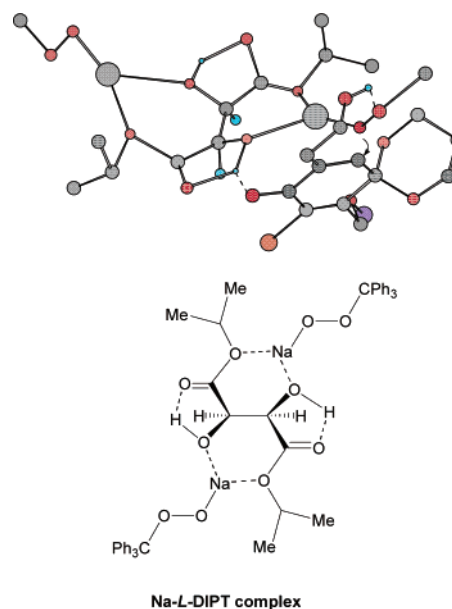
^a Reagents and conditions: (a) (2R, 4R)-pentanediol, PPTS, PhH, 70 °C, 30 min, 82%; (b) Ph₃COOH, KHMDS, THF, −35 °C, 25 h, 73%; (c) NMO, OsO₄, Acetone/H₂O, 30 h; (d) Pb(OAc)₄, THF, 5 min; (e) PPh₃=C(CH₃)COO^tBu, CH₂Cl₂, −78 °C → −5 °C, 2 h, 60% for three steps; (f) (*E*)-tributyl-1-heptylstannane, Pd(PPh₃)₄, PhCH₃, 110 °C, 3 h, 94%; (g) TBAF/AcOH (1:1), THF, 20 h, 80%; (h) 48% HF, CH₃CN, 0 °C, 10 min, 96%.

nucleophilic epoxidation method, substrate **42** was epoxidized smoothly with high enantioselectivity (91% yield, 91% ee (chiral HPLC)) to afford epoxide **43**. Dess–Martin oxidation of **43** followed by two-carbon homologation provided enoate **44**. Stille reaction of **44**, silyl deprotection (TBAF/AcOH), and acetal hydrolysis proceeded smoothly to afford quinone epoxide **9**, which is ready for the Diels–Alder dimerization protocol. The absolute configuration of **9** was assigned by correlation with material produced by diastereoselective epoxidation of a chiral quinone monoketal (Scheme 8). Dimethoxyketal **28** was converted into epoxide **45** by transketalization with a chiral diol, followed by diastereoselective epoxidation (dr = 100:0).^{23,27b,29} The diastereoselective formation of **45** can be explained by steric blocking of the α-face of the dienone by the axial methyl group in the preferred chair conformer **A**. Installation of the protected



2-methyl-2-butenic acid side chain was accomplished by terminal olefin oxidation to an intermediate aldehyde followed by two-carbon homologation to afford enoate **46**.¹⁰ Stille vinylation of **46**, silyl deprotection (TBAF/AcOH), and acetal hydrolysis proceeded smoothly to afford nonracemic quinone epoxide **9** (β-epoxide). Compound **9** produced using both protocols showed comparable optical rotations (**9** (Scheme 8): $[\alpha]_D^{23} = +59.3^\circ$ ($c = 1.0, \text{CHCl}_3$), **9** (Scheme 7): $[\alpha]_D^{23} = +59.2^\circ$ ($c = 0.5, \text{CHCl}_3$)) and thus confirmed the absolute configuration of **9** produced using the tartrate-mediated nucleophilic epoxidation protocol.

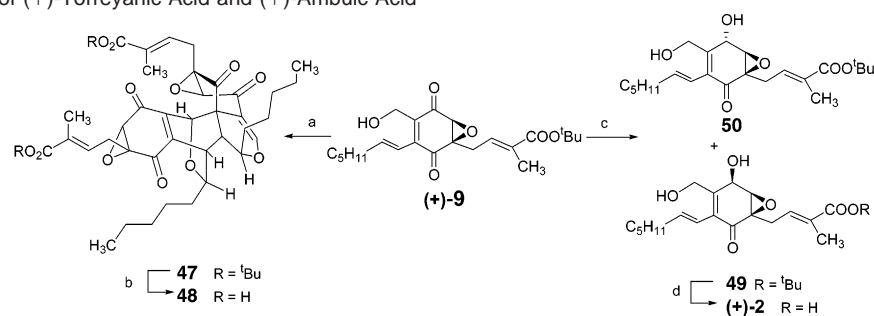
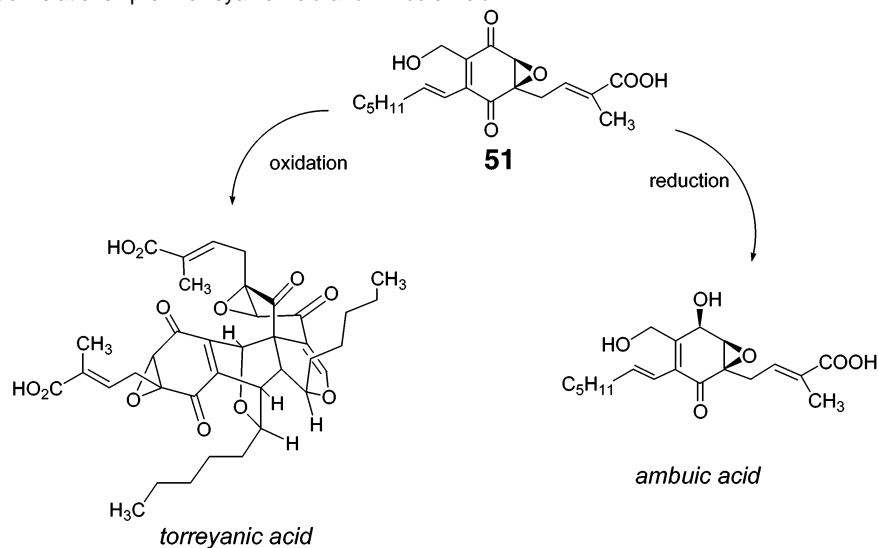
In view of this stereochemical correlation, we suggest a mechanistic proposal for tartrate-mediated nucleophilic epoxidation of homoallylic alcohol substrate **42** as shown in Figure 10. In accord with our proposed model,¹² the asymmetric epoxidation may be facilitated by hydrogen-bond-directing influence between the homoallylic alcohol and the peroxide

**Figure 10.** Mechanistic proposal for hydroxyl-directed asymmetric nucleophilic epoxidation.

oxygen,⁴⁵ which may help anchor the substrate to the putative bowl-shaped chelate.

Final steps toward (+)-torreyanic acid are shown in Scheme 9. Dess–Martin oxidation of (+)-**9** (CH₂Cl₂, 1 h) initiated the tandem oxidation/electrocyclization/dimerization process to afford a single dimeric product **47** (80%), which confirmed the prediction advanced earlier (cf. Figure 6). Treatment of **47** with TFA/CH₂Cl₂ effected *tert*-butyl ester removal to afford **48**. The structure of **48** was confirmed to be identical to natural torreyanic acid by ¹H and ¹³C NMR, IR, TLC *R_f* values (in three solvent systems) and $[\alpha]_D$ (natural: $[\alpha]_D = +92.3^\circ$, $c = 0.11, \text{MeOH}$; synthetic: $[\alpha]_D = +88.2^\circ$, $c = 0.4, \text{MeOH}$). The absolute configuration of natural (+)-torreyanic acid was thus determined to be **48**, the antipode of **1**, and therefore in the same enantiomeric series as the antiangiogenesis agents epoxyquinol A and B (Figure 1).

Finally, we also accomplished the synthesis of the monomeric epoxyquinoid (+)-ambuic acid⁵ from intermediate (+)-**9** (Scheme

Scheme 9. Syntheses of (+)-Torreyanic Acid and (+)-Ambuic Acid^a**Scheme 10.** Biosynthetic Relationship of Torreyanic Acid and Ambuic Acid

9). Reduction of (+)-**9** using NaBH₄/MeOEtEt₂⁴⁷ afforded *syn*-epoxyquinol **49** and epimer **50** in a 1.2:1 ratio. Attempted reduction using a variety of borohydride reagents (LiEt₃BH, LiEt₃BH/MeOEtEt₂, NaBH₄, NaBH(OAc)₃/MeOEtEt₂) did not lead to observable increases in diastereoselectivity. Final deprotection of **49** with HF/CH₃CN gave (+)-ambuic acid **2**. The structure of **2** was confirmed to be identical to natural ambuic acid by ¹H and ¹³C NMR, IR, TLC *R_f* values (in three solvent systems) and [α]_D (natural: [α]_D = +92.1°, *c* = 1.0, MeOH; synthetic: [α]_D = +93°, *c* = 1.0, MeOH). In addition, recent stereochemical analysis of ambuic acid by solid-state NMR confirms the *syn* epoxy alcohol relative stereochemistry determined in this study.⁴⁸ Since natural torreyanic acid and ambuic acid possess the same epoxide chirality, it is likely that both natural products are produced by either oxidation or reduction of quinone epoxide **51** or a related derivative (Scheme 10).

Conclusions

In summary, the first total synthesis and absolute stereochemical assignment of the quinone epoxide dimer (+)-torreyanic acid has been accomplished by employing a [4 + 2] dimerization of diastereomeric 2*H*-pyran monomers. Synthesis of the related monomeric natural product (+)-ambuic acid has also been achieved, which establishes the biosynthetic relation-

ship between these two natural products. A tartrate-mediated nucleophilic epoxidation involving hydroxyl group direction facilitated the asymmetric synthesis of the key chiral quinone monoepoxide intermediate. Thermolysis experiments have also been conducted on a model dimer based on the torreyanic acid core structure and facile retro Diels–Alder reaction processes and equilibration of diastereomeric 2*H*-pyrans have been observed. Higher-temperature thermolysis of the model dimer led to the production of a novel monomeric compound by an apparent pericyclic cascade involving retro [4 + 2], electrocyclic ring-opening, 1,7-hydride shift, and final disrotatory 6π-electrocyclization. In addition, theoretical calculations of Diels–Alder transition states have been performed to evaluate alternative transition states for Diels–Alder dimerization of 2*H*-pyran quinone epoxide monomers and provide insight into the stereocontrol elements for these reactions. Continued studies concerning torreyanic acid and related dimeric and monomeric epoxyquinoid compounds and applications of tartrate-mediated asymmetric nucleophilic epoxidation are in progress and will be reported in due course.

Acknowledgment. Financial support from Boston University and the American Cancer Society (RSG-01-135-01, J.A.P., Jr.) is gratefully acknowledged. We thank Dr. Emil Lobkovsky (Cornell University) for X-ray structure analyses, Professor Gary Strobel (Montana State University) for supplying samples of

(47) Chen, K.-M.; Hardmann, G. E.; Prasad, K.; Repic, O.; Shapiro, M. J. *Tetrahedron Lett.* **1987**, 28, 155.

(48) Harper, J. K.; Barich, D. H.; Hu, J. Z.; Strobel, G. A.; Grant, D. M. J. *Org. Chem.* **2003**, 68, ASAP, Web Release Date: January 24, 2003.

natural torreyanic and ambuic acids, Dr. James Harper (University of Utah) for providing a preprint of their paper, and Professor John Snyder (Boston University) for helpful discussions.

Supporting Information Available: Complete experimental procedures and spectral data for all previously unreported compounds described herein, including X-ray crystal structure

coordinates for **28**, **29**, **33**, and **36**, Cartesian coordinates for calculated Diels–Alder transition states, and NMR spectra for selected compounds (PDF). X-ray crystallographic file in CIF format. This material is available free of charge via the Internet at <http://pubs.acs.org>.

JA021396C